

# Investigating Low-Temperature Hydrothermal Alteration in Drill Cuttings From Pilgrim Hot Springs, Alaska, Using a Suite of Low Cost Analytical Techniques

Joshua K. Miller<sup>1</sup>, Christian Haselwimmer<sup>2</sup>, and Anupma Prakash<sup>2</sup>

<sup>1</sup> Department of Geology and Geophysics, University of Alaska Fairbanks

<sup>2</sup> Geophysical Institute, University of Alaska Fairbanks

## Keywords

*Exploration, low-temperature, reflectance spectroscopy, methylene blue, XRD, hydrothermal alteration, low cost*

## ABSTRACT

Reflectance spectroscopic, methylene blue, and X-ray diffraction (XRD) analyses have been applied to ~400 m of drill cuttings and core from an exploration well at Pilgrim Hot Springs, Alaska with the aim of rapidly characterizing the extent and style of low-temperature hydrothermal alteration as well as determining paths of geothermal fluid-flow. Sample reflectance spectra indicate a mineral assemblage comprised predominantly of montmorillonite, illite, chlorite, and kaolinite with depth-related variations in mineral assemblages, specifically in core section, related to changing alteration intensity. The observations from reflectance spectroscopy show good agreement with the results of methylene blue analyses concerning the distribution of smectite within the cuttings and core samples. The results of XRD for a limited set of the drill cuttings show reasonable agreement with the outcomes of reflectance spectroscopy and methylene blue analyses. The results of this study reveal a history of hydrothermal activity at Pilgrim Hot Springs characterized as argillic alteration. This points to a possible temperature- and chemical-regime elevated above current conditions. The combination of these low-cost techniques can be applied to various geothermal systems as a means of investigating the degree of alteration in sediments and bedrock to determine past hydrothermal fluid migration pathways.

## 1. Introduction (Location Map)

Pilgrim Hot Springs is located ~60 km north of Nome and ~200 km south of the Arctic Circle. The surface expression of the geothermal anomaly encompasses an area of ~1.5 km<sup>2</sup> with groves of cottonwoods and abundant wildflowers despite the surrounding tundra landscape lying on discontinuous permafrost. With 91°C well temperatures recorded at depths as shallow as 12 m, Pilgrim Hot Springs is the hottest known geothermal

system in Interior-Western Alaska (Turner et al., 1980). Results from previous studies have concluded that the system is fluid-dominated and alkali-chloride rich with fluid geochemistry estimates of a deeper reservoir temperature of 150°C (Turner et al., 1980; Liss and Motyka, 1994). Total heat flux has been estimated using a reservoir simulation model at 26 MW (Chitambakkam et al., 2013).

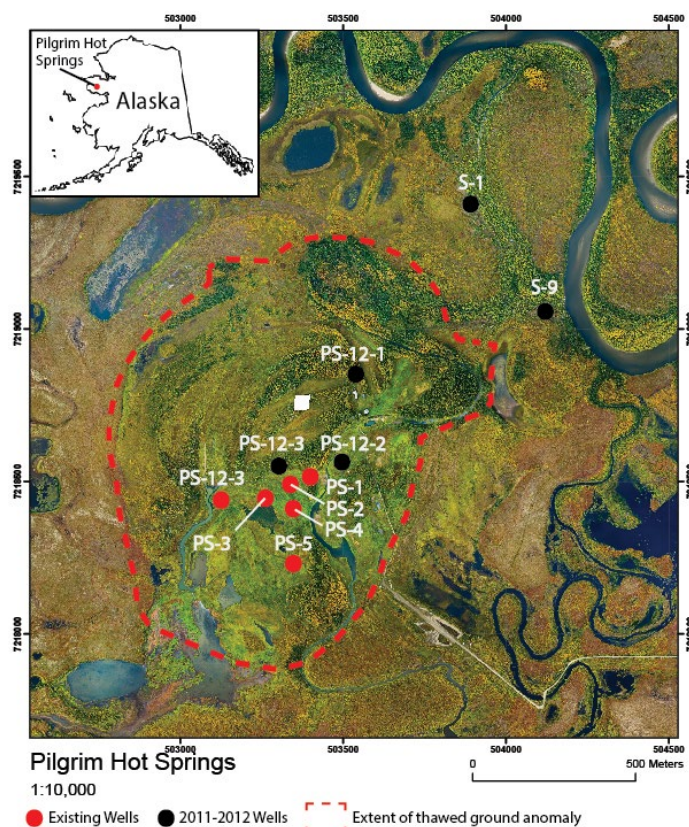


**Figure 1.** Pilgrim Hot Springs, Alaska, located in central Seward Peninsula, with the Pilgrim River in the top half of the map. The ~1.5 km<sup>2</sup> surface anomaly is outlined in red. PS-12-2, located near the center, is the focus of this study.

The viability of the Pilgrim Hot Springs geothermal system (Fig. 1) as a source of small-scale electricity production is currently being assessed by the University of Alaska Fairbanks. The goal is to provide power for the city of Nome or direct-use applications at the hot springs. Exploration of this geothermal site has been conducted since 1979 and was the first to be extensively explored in Alaska (Turner et al., 1980). Beginning in 2010, the Alaska Center for Energy and Power and the Geophysical Institute of the University of Alaska Fairbanks are testing the application of forward looking infrared radiometry (FLIR) remote sensing to reduce the cost of preliminary geothermal exploration by surveying elevated heat loss at the surface of Pilgrim Hot Springs (Daanen et al., 2012; Haselwimmer et al., 2011). Recent exploration drilling has produced five new slimholes; PS-12-2 is the deepest borehole at 400 m intercepting ~80 m of bedrock (Fig. 1).

The purpose of this study was to investigate the extent and magnitude of hydrothermal alteration in the sediments and core from PS-12-2 through the combined use of relatively rapid and low-cost methods that included reflectance spectroscopy, methylene blue analysis, and XRD. Reflectance spectra were used to determine alteration mineral assemblages and absorption feature parameters (e.g. depth and wavelength position of AIOH absorption feature) relevant to hydrothermal alteration style and intensity. Methylene blue analysis was conducted on the more clay-rich drill cuttings to determine the smectite percent. Selected samples from a distinct clay zone in PS-12-2 were oriented and analyzed using XRD to determine the specific clay mineralogy. The outcomes of these analytical techniques were interpreted with reference to existing well lithologic log data to determine zones of hydrothermal alteration and possible pathways of geothermal fluid migration. We aimed to establish correlations between the results of the different analytical methods to facilitate their interpretation and enable extrapolation of the results of methylene blue and XRD analysis.

### 1.1 Geologic Setting

Pilgrim Hot Springs lies a few meters above sea level within a predominantly alluvial basin bounded 5 km to the south by the Kigluaik Mountains and 5 km to the north by Marys Mountain and Hen and Chicken Mountain. The valley is underlain by a Precambrian mica schist graben and Jurassic-Cretaceous felsic to mafic dikes exposed in outcrops in the nearby mountains (Till et al., 2011). The Kigluaik range-front fault at the northern base of the mountain has been previously mapped as a normal fault in a strongly extensional setting (Ruppert et al., 2008; Turner et al., 1980).

Stratigraphic studies indicate the presence of several significant clay intervals in the geothermal system that act as a clay cap

to the deeper reservoir within the bedrock (Miller et al., 2013). A shallow outflow aquifer is present in indurated silts and sands and lenses of fluvial gravels from 30-90 m depth with 91°C temperatures. At 90-120 m, a temperature reversal located in higher permeability sands/gravels is seen as a result of cold groundwater influx to the system. Increasing temperature gradients up to 91°C within the sediments, high outflow temperatures, and a vertical zone of indurated sediments suggest an upflow in close proximity to PS-12-2 and PS-12-3.

The focus of this study is the alteration of sediments and bedrock, particularly in PS-12-2, to infer the nature and extent of the hydrothermal alteration of this geothermal system as well as a means of testing the agreement of these methods by further characterizing the reservoir. Samples selected for analysis consist of unconsolidated to poorly indurated silt-gravels, clays, and 15 m of core. Thin-section characterization of the core (Fig. 2) indicates this consists of a biotite schist intruded by pegmatite and diabase dikes.

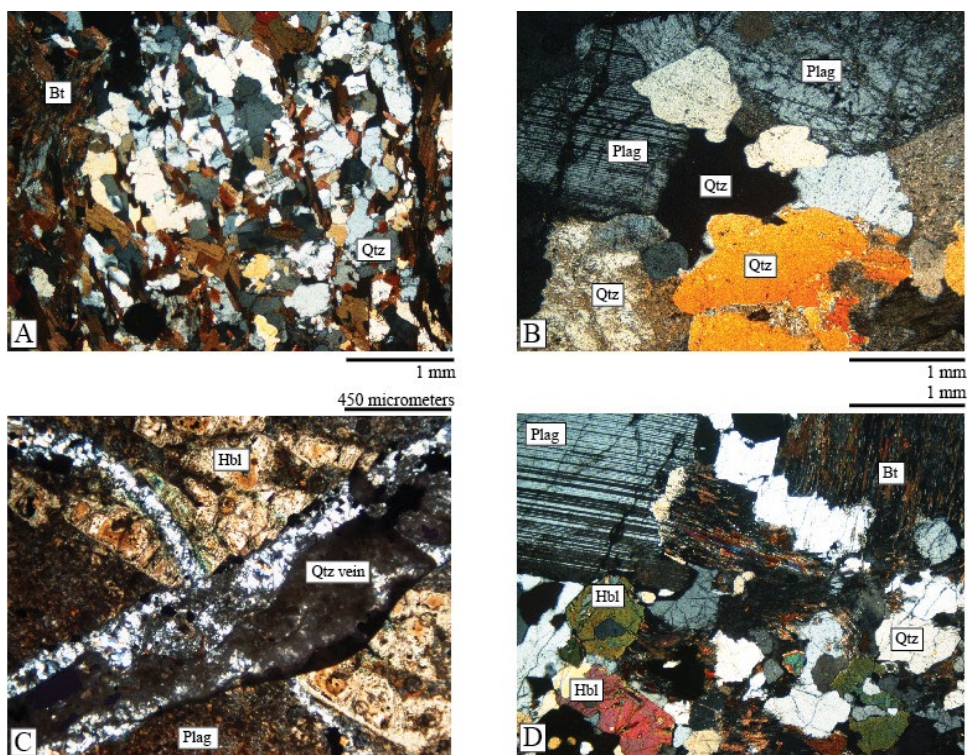


**Figure 2.** Thin section images from PS-12-2 core. All images are under crossed polars. [A] Representative sample of the biotite (Bt) schist. Minor alteration is present in some biotites. [B] Pegmatitic dike with large plagioclase (Plag) and quartz (Qtz). [C] Diabase dike with a 3 mm hornblende (Hbl) crystal cut by two quartz veins with a groundmass of plagioclase. Mineral degradation and the early stages of hornblende replacement by quartz are visible. [D] Contact of the pegmatitic dike and biotite schist. Hornblende, quartz, plagioclase, and biotite are common. The biotites appear altered at the contact. Fine-grained pyrite (only discernible in reflected light) is very common as a replacement mineral along the dike-schist contact.

## 2. Methods

### 2.1. Reflectance Spectroscopy

Visible to shortwave infrared (VNIR-SWIR) reflectance spectra were acquired over the 400-2500 nm wavelength region with an ASD FieldSpec Pro and a high-intensity contact probe

using a white Spectralon panel as reference. In the VNIR-SWIR wavelength region hydroxyl, hydrate, and carbonate anions as well as transition elements (dominantly iron) produce distinctive absorption features (Hunt, 1977). These spectral features can be used to investigate mineralogical properties related to hydrothermal alteration such as alteration mineral assemblages or variations in specific mineral chemistry, which may be related to changing alteration conditions. For example, the depths and wavelength positions of absorption features, such as those related to AlOH and FeOH bonds, can be utilized as proxies for the extent and magnitude of hydrothermal alteration (Calvin et al., 2010; Haest et al., 2012; Harraden et al., 2013; Ruitenbeek et al., 2005).

In this work we compiled the acquired spectra into a hyperspectral image cube that stacks spectral data, in this case, against sample depth, to provide a convenient method for data visualization (Fig. 3). In total, 400 spectra from the sediments samples were used in addition to 265 spectra of the 15 m core section taken at six cm intervals. Using the ENVI software package, RGB false color composites focused on specific mineral absorption features were produced to qualitatively investigate the range of mineral assemblages and variation in alteration intensity with depth. A continuum-removal procedure (Clark and Roush, 1984) was applied to better enhance the depth of specific absorption features as well as removing slope effects on absorption feature wavelength positions. Qualitative interpretation of major spectral classes manifested in the data was undertaken with reference to the USGS Digital Spectral Library (Clark et al., 2007) in order to identify the dominant mineral assemblages (Figure 3). Using scripts implemented in IDL, the continuum-removed depth and wavelength position of major mineral absorption features in the VNIR-SWIR was determined from the spectral data. The scripts were based on procedures adapted from Haest et al. (2012) that involved fitting polynomial curves of various orders of magnitude to the continuum-removed spectra for different absorption features. The resultant spectral parameters were used to determine specific mineral assemblages following the procedures outlined by Haest et al. (2012) as well as providing variables that were cross-compared with the results of methylene blue and XRD analyses. Analysis of the sample spectra was also undertaken using The Spectral Geologist (TSG)

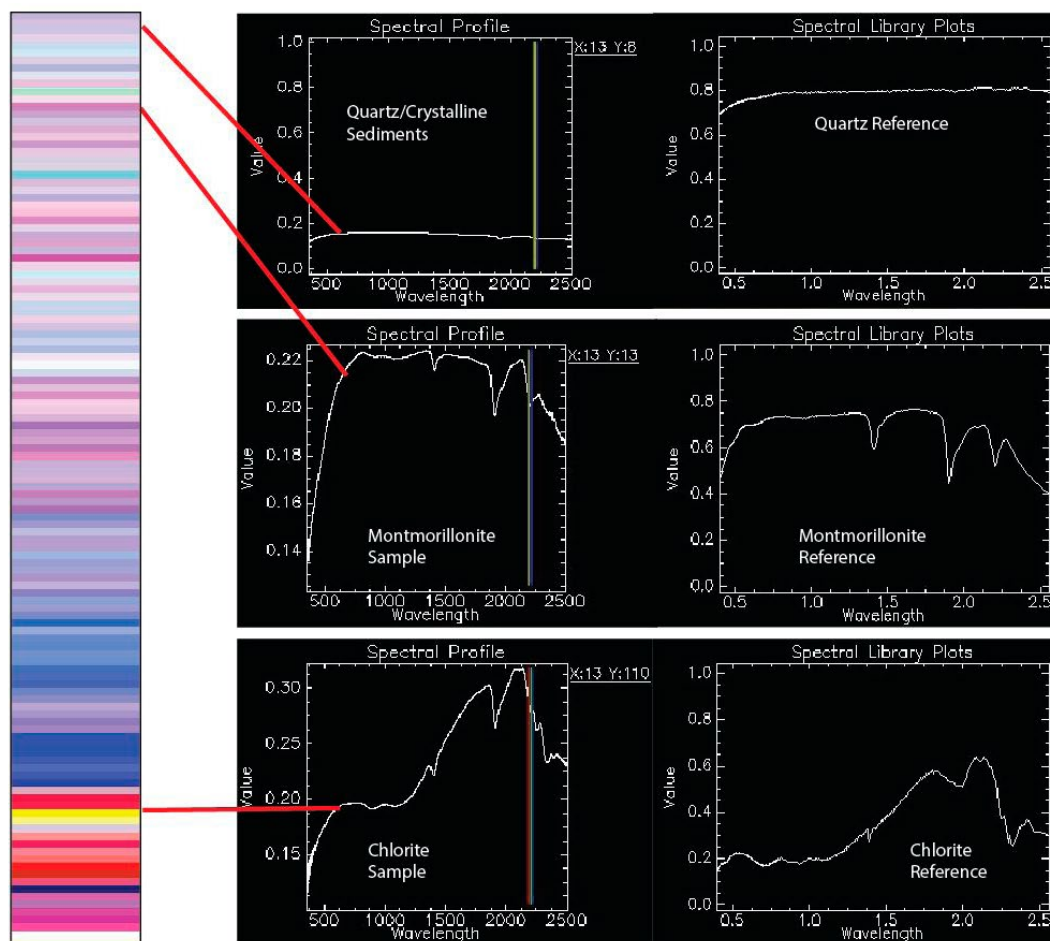


**Figure 3.** Hyperspectral image cube of PS-12-2 with stacked spectra corresponding to sample depth. Reference mineral spectra (USGS Spectral Library) have been selected: montmorillonite (magenta), chlorite (yellow), muscovite (red), illite (blue), and white (assumed to be highly crystalline sediments with quartz as an example). The spectral plots are stacked and continuum removed to highlight the profile subtleties for clarity of comparison. Red (2180 nm), green (2205 nm) and blue (2230 nm) define the ALOH absorption feature to distinguish Al-rich mineral phases by color association as a function of absorption depth. The sample spectra are included to demonstrate the correlation to montmorillonite, chlorite, and unaltered (quartz example) spectral references.

software package to provide an independent check concerning the interpreted mineral assemblages.

## 2.2. Methylene Blue

Methylene blue analysis is a common approach to determining the abundance of smectite and mixed illite-smectite clays (Gunderson et al., 2000). 27 samples were selected at ~15 m intervals from PS-12-2. This analysis requires titration of methylene blue into a saturated sample of clay (Harvey, 1993). The exact smectite mineral is typically ascertained by XRD (Gunderson et al., 2000). In solution, methylene blue is a cationic dye with the molecular structure  $C_{16}H_{18}N_3S^+$  that readily adsorbs onto smectite clays due to their very high cation exchange capacity and hydrogen bonding with the alumino-silicate lattice structure (Santamarina et al., 2002; Yukselen and Kaya, 2008). It is an important application for the assessment of swelling clay content in drill cuttings as it can affect well production by reducing rock stability (Gunderson et al., 2000). Applying methylene blue analysis to clay-rich drill cuttings can be compared to zones of low resistivity detected in geophysical surveys and delineate areas of possible high-temperature altera-

tion in association with the migration of geothermal fluids as a geothermometer (Gunderson et al., 2000; Harvey and Browne, 2000; Lagat, 2007).

### 2.3 XRD

Four clay samples from 240-300 m depth in PS-12-2 were analyzed using the PANalytical X'PERT PRO Materials Research Diffractometer (MRD) XRD in the Advanced Instrumentation Lab at the University of Alaska Fairbanks. Using a  $\text{CuK}\alpha$  source, the analytical range was from  $2\text{-}59^\circ 2\theta$  with a  $0.01^\circ$  step size and 15 seconds per step. The samples obtained from drill cuttings from PS-12-2 were prepared for oriented clay XRD analysis. The clays were decanted, separated from  $>2\mu\text{m}$  particles, and saturated with a 2 M solution of  $\text{MgCl}_2$  as expanding with an index cation yields predictable results that allow differentiation from other clays (Wilson, 1987). The clays were then oriented in a vacuum filter apparatus and placed on glass slides. Separate XRD runs were completed after air-drying and ethylene glycolation. Expanding clays (e.g. smectites) shift from  $10\text{ \AA}$  after air-drying to  $14\text{ \AA}$  with ethylene glycol treatment (Mosser-Ruck et al., 2005). The results of XRD analysis are compared to the results of the other methods.

## 3. Results

The outcomes of the different analyses indicate an alteration mineral assemblage within the sediments and core comprised of various clays and micas. The reflectance spectroscopy results indicate that the dominant mineral assemblages include the specific smectite mineral montmorillonite and chlorite (Figure 3). The absorption features of OH at  $1400\text{ nm}$ ,  $\text{H}_2\text{O}$ , at  $1900\text{ nm}$ , and specifically the AIOH absorption feature at  $2205\text{ nm}$  with shoulder peaks at  $2160\text{ nm}$  and  $2240\text{ nm}$  are strong indicators of montmorillonite. The interpretation of montmorillonite is also supported by methylene blue analysis suggesting smectite content up to 10% per gram of sample and XRD analysis (Fig. 5) reveals that the smectite is montmorillonite. Chlorite was identified by low reflectance in the visible spectrum, the multiple absorptions in the  $\text{H}_2\text{O}$  band, and a small AIOH absorption on the shoulder of the much more pronounced FeOH band at  $2250\text{ nm}$  and MgOH band from  $2330\text{-}2450\text{ nm}$ . Although detectable in XRD, kaolinite was not easily distinguished in the spectral analysis. The USGS library spectra for montmorillonite-kaolinite (12%) offered the closest resemblance to sample spectral profiles, but this particular mineral assemblage is almost indistinguishable from pure montmorillonite reference spectra.

To further characterize the extent of alteration within the samples, the White Mica Alteration Index (WMAI) was calculated. This is the ratio of the AIOH absorption depth of white mica to the depth of the FeOH absorption feature in chlorite (Van Ruitenbeek et al., 2005); the ratio increases with white mica relative to the abundance of chlorite. WMAI values that plot higher than .75 are interpreted to be mostly white mica while chlorite dominates the lower half at .5 and below (Van Ruitenbeek et al., 2005). The relative Al content of the white micas determines the wavelength position of the AIOH absorption feature and changes with temperature, hydrothermal fluid chemical substitution, and the mineral composition of the host rock type (Van Ruitenbeek et al., 2005).

Figure 3 is a WMAI scatter plot of wavelength values within  $2190\text{-}2215\text{ nm}$  which is the characteristic range of the AIOH absorption band. The WMAI for the sediments tend to exhibit a relatively low Al content possibly as a result of increased temperature ( $100^\circ\text{C}$ ) or evolving hydrothermal fluid chemistry (Van Ruitenbeek et al., 2005). The deeper sediments and shallow basement surface rock cuttings plot in the chlorite dominant range that suggests a more pronounced alteration of the mica schist. The core displays a wide spectrum of variable white mica-chlorite values. TSG results indicate the abundance of (Fe,Mg) chlorite relative to a lesser amount of white micas such as muscovite and paragonite.

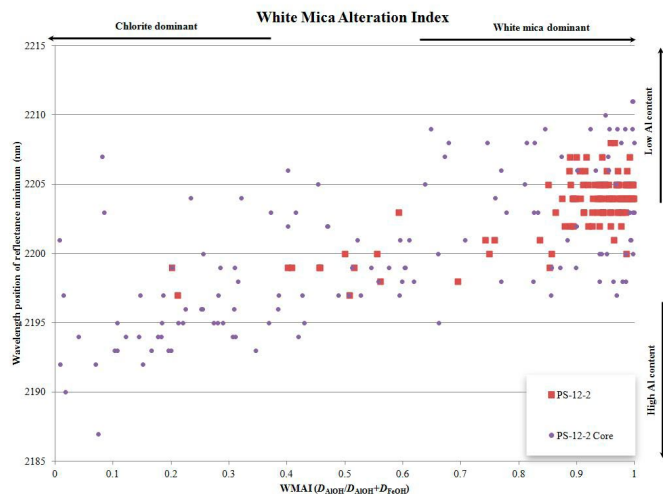


**Figure 4.** White Mica Alteration Index (WMAI) scatter plot for PS-12-2 AIOH and FeOH absorption feature depth and wavelength position changes.

The common minerals detected in the XRD results (Fig. 5) include abundant montmorillonite, common illite/chlorite, kaolinite, and minor biotite. Peak matches within the  $2\text{-}59^\circ 2\theta$  range and respective d-spacings for known minerals show a strong match with montmorillonite clay. Peak position and count intensity matches with other minerals may be slightly variable as the samples were oriented with the C-axis of the clays preferentially aligned. Thus, correlations to peaks of other mineral structures at a specific  $^\circ 2\theta$  are limited to the 001 line. Peaks on other lines and orientations may not show up. When considering a mineral identification, this orientation served as a mechanism for filtering out other mineral structures by looking at database results of measured  $^\circ 2\theta$  angles and d-spacing values at the 001 line. Also, the charge difference of these particular clay samples may not be the same as the reference samples which would result in count intensity,  $^\circ 2\theta$ , and d-spacing offsets.

In Figure 5, a strip log of PS-12-2 and temperature log are compared to the AIOH absorption depth, methylene blue, hyperspectral cube, and TSG mineral assessments. XRD results are used to validate the results of the methylene blue analysis.  $0\text{-}150\text{ m}$  depth, with a corresponding increase in temperature from outflowing fluids, is comprised mainly of montmorillonite and muscovite. The hyperspectral cube shows a strong montmorillonite zone at  $\sim 30\text{ m}$  depth (white).  $150\text{-}230\text{ m}$  is marked by an increase in methylene blue estimates of smectite content up to 8%. AIOH absorptions generally increase in depth which

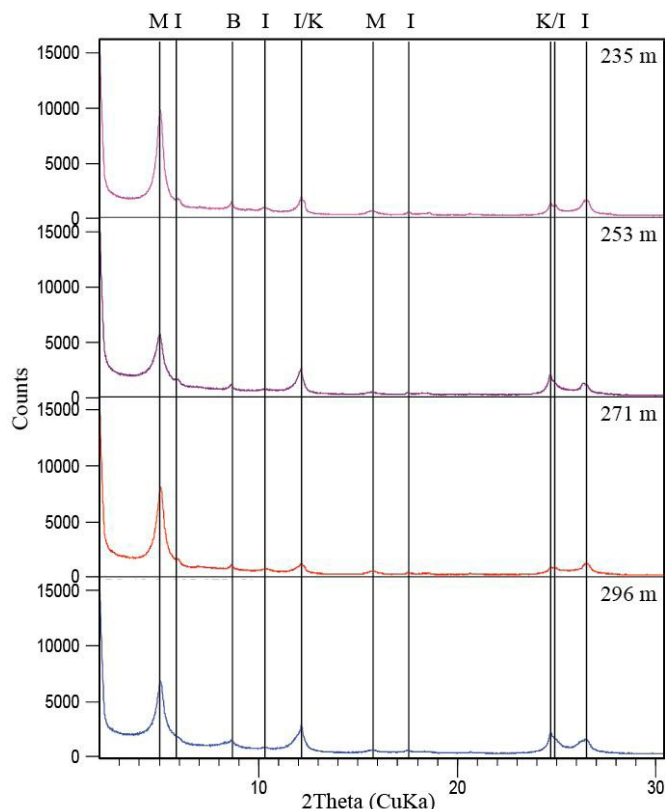
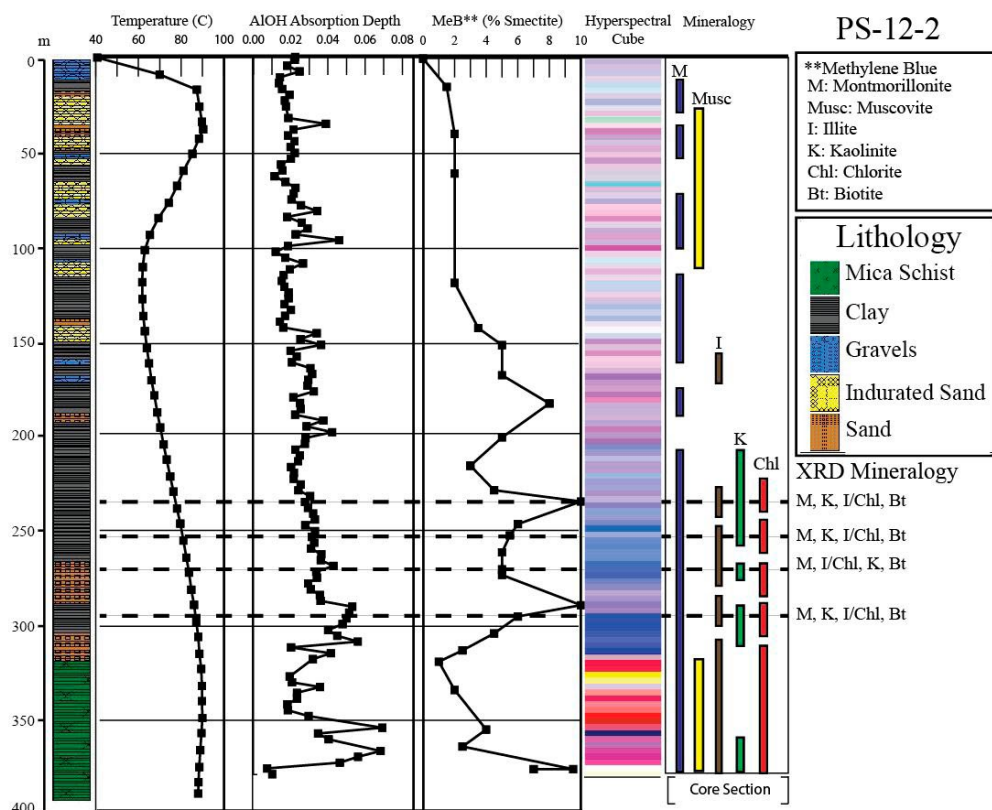


**Figure 5.** XRD patterns of (M) Montmorillonite, (I) Illite, (K) Kaolinite, (B) Biotite from depths of 235-296 m. The clay samples were oriented and saturated with ethylene glycol. Results are dominated by montmorillonite with variable abundances of illite and kaolinite composition and minor biotite.

corresponds to montmorillonite in the hyperspectral cube. Also, montmorillonite-illite is present at a zone with gravel lenses that could be related to alteration associated with the influx of hot fluids through these permeable layers. The depths from 230-300 m are characterized by an abrupt montmorillonite zone (up to 10% smectite) as indicated by increasing AIOH depths. This trend of increasing AIOH depths occurs where TSG software also detected kaolinite, an aluminosilicate mineral. Good agreement between XRD and TSG mineralogy reveal dominant montmorillonite, common kaolinite, illite/chlorite, and minor biotite. The region from 300-375 m defines the transition from sediment to basement at which the AIOH feature displays an erratic trend in response to the loss of kaolinite and increase in chlorite and muscovite.

**Table 1.** The Spectral Geologist (TSG) spectral analysis mineral results for PS-12-2 sediments and core. Results are listed from most abundant to least abundant.

PS-12-2 Sediments	PS-12-2 Core
Montmorillonite	FeMgChlorite
Kaolinite	Phlogopite
Siderite	MgChlorite
FeMgChlorite	Montmorillonite
Muscovite	Palygorskite
Aspectral	Muscovitic Illite
Palygorskite	Muscovite
Ankerite	Calcite
Magnesite	Siderite
Muscovitic Illite	Ankerite
MgChlorite	Biotite
	Hornblende



## Discussion

The mineral assemblage of the sediment-basement contact and bedrock core is common for geothermal systems which includes montmorillonite, illite, chlorite, as well as a host of accessory minerals that have been identified using TSG (Table 1) (Browne, 1978). Alteration seen in thin-sections of the core is limited to altered biotites at or near dike contacts, pyritization in quartz veins and mineral contacts, and hornblende replacement by quartz in the deeper diabase dike sections. Distinct minerals often seen in high-temperature systems are absent. However, the cored section is only 15 m and represents the shallow basement composition. Deeper depths may reveal a more compelling story of the history of alteration at the site.

**Figure 6.** PS-12-2 striplog, temperature, AIOH absorption depths, methylene blue, hyperspectral cube, and mineralogy as assessed by TSG spectroscopy, and XRD.

The alteration mineral assemblages of white micas and clays dominated by kaolinite, montmorillonite, and illite observed from PS-12-2 are consistent with argillic alteration facies. These minerals are commonly associated with hydrothermal alteration in geothermal systems and have previously been utilized as geothermometers due to the varying stability of different assemblages of these minerals as a function of temperature, depth, fluid and rock chemistry (Browne, 1978; Henley and Ellis, 1983; Reyes, 1990; Gunderson *et al.*, 2000; Harvey and Browne, 2000). The presence of kaolinite indicates an environment of necessary temperature <180°C and low pH conditions required to strip the alkalis from muscovites as well as iron, calcium, and magnesium from montmorillonite through the process of hydrolysis (Guilbert and Park, 1986; Reyes, 1990). Montmorillonite is a common alteration product in many fossil hydrothermal systems and in argillic alteration zones in ore deposits (Guilbert and Park, 1986; Henley and Ellis, 1983). The overall abundance of montmorillonite typically decreases with depth and increasing temperature as it occurs as a shallow feature of most geothermal systems (Browne, 1978; Reyes, 1990). Diagenetic illite is progressively interlayered with montmorillonite with increasing depth and temperature (Jennings and Thompson, 1986). Authigenic illite requires much higher temperatures at 200-220°C for crystallization (Browne, 1978; Henley and Ellis, 1983; Jennings and Thompson, 1986; Reyes, 1990). Chlorite, as a swelling clay, has been described to reach equilibrium at a wide range of temperatures from 125°C-200°C (Browne, 1978; Jennings and Thompson, 1986; Lagat, 2007; Reyes, 1990).

The assemblage of these minerals in PS-12-2 suggest a past equilibrium temperature of 125-180°C. Kaolinite, chlorite, and the dominance of montmorillonite over illite constrain the temperature estimation. Although abundant chlorite and a range of carbonates are listed in the TSG results, it is possible the high-temperature late-stage Jurassic dike intrusions into the basement may have had more impact on mineralizing the shallow basement than hydrothermal processes of the Pilgrim geothermal system. The absence of higher temperature alteration above the threshold of interlayered illite-smectite clays in the sediments also supports this hypothesis. Regardless, extensive pyritization and a mineral assemblage that suggests argillic alteration is present in both the core and sediments which point to a possible temperature- and chemical-regime elevated above current conditions of hydrothermal activity at Pilgrim Hot Springs and could allude to the nature of the heat source. Resolving the past temperature regime into a distinct or multiple distinct thermal events cannot be reliably drawn from the current understanding without further thermochemical studies of the sediments and fluids.

## Conclusions

These seemingly different tests as a whole show good agreement in cross-comparison in exploring the extent of hydrothermal activity at Pilgrim Hot Springs. Overlap occurs in areas of significant mineralogical changes either by increases in methylene blue estimates of smectite content, changes in absorption feature depths, or the appearance/disappearance of particular minerals. These low cost methods can be applied to various geothermal systems as a means to quickly assess the degree of alteration in

sediments and bedrock to determine past hydrothermal fluid migration pathways. In the case of Pilgrim Hot Springs, these methods have enabled the recognition of several diagnostic minerals that resemble argillic alteration which suggests past temperatures up to 180°C. Future work includes applying these methods to the other wells on site as well as applying statistical analysis methods to the combined spectral, methylene blue, and XRD dataset. Also, to better understand the thermal history of Pilgrim Hot Springs, a fluid inclusion homogenization temperature study would provide past subsurface temperatures.

## Acknowledgement

I would like to acknowledge and thank Dr. Franta Majs and Dr. Tom Trainor at the Advanced Instrumentation Lab at the University of Alaska Fairbanks for the guidance in XRD analysis, Susana Jaramillo for procedural help in clay preparation, and William Cumming for direction in methylene blue analysis. This work is funded by the Department of Energy Geothermal Technologies Programme (CID: DE-EE0002846) and Alaska Energy Authority Renewable Energy Fund Round III.

## References

- Browne, P. R.L., 1978, Hydrothermal alteration in active geothermal fields, *Annual review of earth and planetary sciences*, v. 6, p. 229-250.
- Calvin, W., Lamb, A., Kratt, C., 2010, Rapid Characterization of Drill Core and Cutting Mineralogy using Infrared Spectroscopy, *Geothermal Resource Council Transactions*, v. 34, p. 761-764.
- Chittambakkam, A. Daanen, R. P., Haselwimmer, C., Prakash, A., Holdmann, G., 2013, Development of a Reservoir Stimulation Model at Pilgrim Hot Springs, Alaska using Tough2, *Proceedings, Thirty-eighth Workshop on Geothermal Reservoir Engineering*, Stanford University, Stanford, California, Feb 11-13, 2013, SGP-TR-198.
- Clark, R.N., Swayze, G.A., Wise, R., Livo, E., Hoefen, T., Kokaly, R., Sutley, S.J., 2007, USGS digital spectral library splib06a: U.S. Geological Survey, *Digital Data Series 231*.
- Daanen, Ronald P., Chittambakkam, Arvind, Haselwimmer, Christian, Prakash, Anupma, Mager, Markus, Holdmann, Gwen, 2012, "Use of COMSOL Multiphysics to Develop a Shallow Preliminary Conceptual Model for Geothermal Exploration at Pilgrim Hot Springs, Alaska," *Geothermal Resource Council Transactions*, v. 36, p. 631-635.
- Guilbert, J.M., Park, Jr., C.F., 1986, *The Geology of Ore Deposits*, Waveland Press, Long Grove, Illinois.
- Gunderson, R., Cumming, W., Astra, D., Harvey, C., 2000, Analysis of Smectite Clays in Geothermal Drill cuttings by The Methylene Blue Method for well site geothermometry and resistivity sounding correlation, *Proceedings, World Geothermal Congress, Kyushu-Tohoku, Japan*, p. 1175-1181.
- Haest, M., Cudahy, T., Laukamp, C., Gregory, S., 2012, Quantitative mineralogy from infrared spectroscopic data. I. Validation of mineral abundance and composition scripts at the Rocklea Channel iron deposit in Western Australia, *Economic Geology*, v. 107, p. 209-228.
- Harraden, C.L., McNulty, B.A., Gregory, M.J., Lang, J.R., 2013, Shortwave Infrared Spectral Analysis of Hydrothermal Alteration Associated with the Pebble Porphyry Copper-Gold-Molybdenum Deposit, Iliamna, Alaska, *Economic Geologist*, v. 108, p. 483-494.
- Harvey, C., 1993, Simplified Methylene Blue Test for Estimation of Swelling Clays, *GNS Science*, Annotated by W. Cumming, 2004 and 2010.
- Harvey, C., Browne, P., 2000, Mixed-Layer Clays in Geothermal Systems and their effectiveness as Mineral Geothermometers, *Proceedings World Geothermal Congress 2000, Japan, May 28-June 10, 2000*.

- Haselwimmer, C., Prakash, A., Holdmann, G., 2011, "Geothermal Exploration in Pilgrim, Alaska Using Airborne Thermal Infrared Remote Sensing," *Geothermal Resource Council*, 35th Annual Meeting, Oct 23-26, San Diego, California.
- Henley, R.W., Ellis, A.J., 1983, Geothermal systems ancient and modern: a geochemical review, *Earth-Science Reviews*, v. 19, p. 1-50.
- Hunt, Graham R., 1977, Spectral Signatures of Particulate Minerals in the Visible and Near Infrared, *Geophysics*, v. 42, n. 3, p. 501-513.
- Jennings, S., Thompson, G.R., 1986, Diagenesis of Plio-Pleistocene sediments of the Colorado River Delta, Southern California, *Journal of Sedimentary Petrology*, v. 56, no. 1, p. 89-98.
- Lagat, John, 2007, Hydrothermal Alteration Mineralogy in Geothermal fields with case examples from Ollkaria Domes Geothermal Field, Kenya, Short Course II on Surface Exploration for Geothermal Resources, UNU-GTP and KenGen, Kenya, November 2007.
- Liss, S.A., Motyka, R.J., 1994, Pilgrim Springs KGRA, Seward Peninsula, Alaska: Assessment of Fluid Geochemistry, *Geothermal Resources Council Transactions*, v. 18, p. 213-219.
- Mas, A., Guisseau, D., Mas, P. Patrier, Beaufort, D., Genter, A., Sanjuan, B., Girard, J.P., 2006, Clay minerals related to hydrothermal activity of the Bouillante geothermal field (Guadeloupe), *Journal of Volcanology and Geothermal Research*, v. 158, p. 380-400.
- Mosser-ruck, R., Devineau, K., Charpentier, D., Cathelineau, M., 2005, Effects of Ethylene Glycol Saturation Protocols on XRD Patterns: A Critical Review and Discussion, *Clays and Clay Minerals*, v. 53, no. 6, p. 631-638.
- Reyes, Agnes, G., 1990, Petrology of Philippine geothermal systems and the application of alteration mineralogy to their assessment, *Journal of Volcanology and Geothermal Research*, v. 43, p. 279-309.
- Ruppert, N.A., 2008, Stress map for Alaska, *Geophysical Monograph Series*, v. 179, edited by J. T. Freymueller et al., p. 351-367.
- Santamarina, J.C., Klein, K.A., Wang, Y.H., Prencke, E., 2002, Specific surface: determination and relevance, *Canadian Geotechnical Journal*, v. 39, p. 233-241.
- Till, Alison B., Dumoulin, J. A., Weldon, M. B. Bleick, H. A., 2011, Bedrock Geologic Map of the Seward Peninsula, Alaska, and Accompanying Conodont Data, US Department of the Interior, U. S. Geological Survey.
- Turner, D. L., Forbes, R. B., 1980, A Geological and Geophysical Study of the Geothermal Energy Potential of Pilgrim Springs, Alaska, *Geophysical Institute, University of Alaska*, UAG R-271.
- Van Ruitenbeek, Frank J.A., Cudahy, Thomas, Hale, Martin, Van der Meer, Freek D., 2005, Tracing fluid pathways in fossil hydrothermal systems with near-infrared spectroscopy, *Geology*, v. 33, no. 7, p. 597-600.
- Wilson, M.J., 1987, *A Handbook of Determinative Methods in Clay Mineralogy*, Blackie, Glasgow, Scotland.
- Yukselen, Y., Abidin, K., 2008, Suitability of the methylene blue test for surface area, cation exchange capacity, and swell potential determination of clayey soils, *Engineering Geology*, v. 102, p. 38-45.

